UCRL-ID-149864

Armor Possibilities and Radiographic Blur Reduction for The Advanced Hydrotest Facility

M. Hackett

September 1, 2002

U.S. Department of Energy
Lawrence Livermore National Laboratory

DISCLAIMER

This work was performed under the auspices of the U. S. Department of Energy by the University of California, Lawrence Livermore National Laboratory under Contract No. W-7405-Eng-48.

Acknowledgments

It is a pleasure to acknowledge contributions from a large number of individuals during this investigation. The author would like to offer particular thanks to John Pastrnak, Carl Henning, and Ed Kokko for their helpful insight and guidance throughout the study, their time in reviewing this report was also gratefully appreciated. Thanks are also offered to Peter Barnes who provided tremendous help during the construction and validation of SABR Factors, without his help this tool would still be in development. The author would also like to acknowledge the assistance of Steve DeTeresa, Vern Switzer, Walt Grundler, and Ed Dalder for their contributions. This work was supported by the Defense and Technologies Engineering Division (DTED) at Lawrence Livermore National Laboratory (LLNL).

Abstract

Currently at Lawrence Livermore National Laboratory (LLNL) a composite firing vessel is under development for the Advanced Hydrotest Facility (AHF) to study high explosives. This vessel requires a shrapnel mitigating layer to protect the vessel during experiments. The primary purpose of this layer is to protect the vessel, yet the material must be transparent to proton radiographs. Presented here are methods available to collect data needed before armor selection, along with a comparison tool developed to aid in choosing a material that offers the best of ballistic protection while allowing for clear radiographs.

Introduction

In an effort to gain knowledge about nuclear weapons, dynamic data is collected from tests simulating the fissile materials, nuclear explosions, aging affects and other parameters affecting these weapons. The Advanced Hydrotest Facility (AHF) has been proposed to help collect this data and will use a fairly new method, proton radiography, to do so.

When collecting this dynamic experimental data there are at least two general obstacles, the first is potential damage from the explosives to the equipment and the second is possible contamination of the environment due to hazardous materials in the experiment. To overcome these obstacles contained firing vessels are implemented. Conventional vessels are made of steel and have low-density windows. These windows provide a view of the experiment and allow scientists to collect data using methods such as radiography. The number of windows the vessel contains restricts the number radiographic lines of sight allowable and thus the amount of data to be collected. Currently at Lawrence Livermore National Laboratory (LLNL) a low density composite firing vessel is being designed for the AHF project. This vessel is being designed to contain a blast of 80 lb. of TNT and has a windowless feature to reduce the chance of leakage and allow for any number of radiographic lines of sight. It is being designed for two separate purposes; one is repetitive use with non-nuclear experiments and the other is one time use with special nuclear materials (SNM).

The vessel has a neck region at the top and bottom and is spherical in the middle as shown in figure 1. The diameter across the middle of the spherical region will be about 2 meters and the entire vessel will be made of three layers. The outer layer will

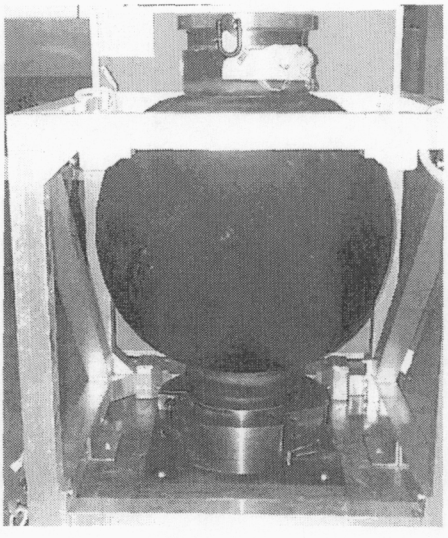

Figure 1: Half scale model of the composite firing vessel under development at LLNL.

consist of a fiber based composite about 4 inches thick. Possible composites are Kevlar or PBO; this layers' main function is to bear some of the load from the experiment. The middle layer will be made of aluminum approximately 2 inches thick and will be similar to 2219, 2024 or 6061-T6 aluminum. The aluminum layer will act as the primary seal to contain noxious gases and all other experimental material. The inner layer is ceramic and its purpose is to protect the aluminum from shrapnel damage in order to prevent a breach in the vessel.

This report discusses the methodology for choosing a ceramic, presents a tool for use in comparing ceramics from a proton radiographic standpoint. It also discusses possible codes for modeling the ceramic as vessel armor and methods of analyzing shrapnel plates.

Methodology of Selection

In order to choose the appropriate ceramic for our vessel a set of comparison criteria have been established. We have consulted with an expert in the field of fracture mechanics, Dr. Mark L. Wilkins, and will soon begin comparing various computer codes that are appropriate for analyzing our problem. This section presents these preliminary steps in detail.

Fragment Characterization

We currently are assuming our threat to be a sphere, 1 cm in diameter, of tungsten. However, the nature of high explosives suggests a large variety of fragments from small and smooth to large and jagged. It is obviously difficult to calculate the exact size, shape and velocity of these fragments, yet an accurate characterization is necessary. Possible methods of collecting data include using a soft non-reacting medium to stop the fragment, such as water or drywall, that will provide information on mass and shape, using x-ray heads to determine the impact velocity and the manner in which the fragment strikes the target, i.e. does it act like a blunt or sharp projectile, and is there a considerable yaw angle?

Currently witness plates of aluminum and in some cases ceramic tile backed by aluminum are used to catch the fragments. Measurements such as length, width, and depth of the craters are then taken from these plates. X-rays are also taken to show the deepest craters and fragments that can not be seen from the surface. Difficulty in collecting data is encountered when craters from different fragments are adjoined preventing accurate measurements. How the witness plate material interacts with the fragment is also unknown, there is a possibility that at the incident velocities the fragments may become pyrophoric and melt their way through the witness plate. We are also unsure of just how many fragments formed. These witness plates may provide more information once x-ray computed tomography and metallography is performed.

X-ray computed tomography (XCT or CT) provides a computerized three-dimensional reconstruction of the witness plate using x-rays to determine the location of voids or inclusions. For a better explanation a section of a report by Amy M. Waters [May 2001] is reproduced below.

"...X-ray computed tomography (CT) was developed as a way to extract the three-dimensional spatial information from two-dimensional projections (radiographs). Computed tomography involves acquiring multiple radiographic projection images of an object at different angles using digital detectors. These projections are processed and mathematically reconstructed using a computer to obtain a 3-D image or representation of the object. For X-ray CT, the final 3-D image is a map of the linear attenuation coefficient that can be examined through specific slice planes of interest.

CT allows for the dimensional spatial information to be readily obtained, including diameters, spatial locations, and thicknesses. Microstructure can be quantified and analyzed using CT, as shown by Taleff, et al. in 2000, Horstemeyer and Gokhale in 1999, Waters, et al. in 1999 and 2000, Martz, et al. in 1999 and many others [Kinney, et al., 1995; 1994]. Taleff, et al., used ultra-high resolution CT to obtain volumetric rendered images of the porosity in an Al-Mg alloy. Because CT data is often volumetric, quantitative 3-D data can be readily obtained and used with finite element analyses."

As described in a previous paper [M. Hackett 2001] there is a 3-step plan to choose the proper ceramic for this vessel. In step one we would like to determine the trend between the size and number of fragments. Theoretically, with a large enough data set, we should be able to extrapolate to the single largest fragment our vessel will see. Next we would like to determine the largest amount of energy deposited in a crater. This becomes a little tricky because a smaller faster fragment can deposit a larger amount of energy than a large slow fragment. Last, we want to know the largest crater depth as related to crater volume. This information would provide a robust characterization of the expected threat and would allow for an accurate description of desirable armor material properties.

Ceramic Characterization

Once the threat is characterized a method of comparing armor is necessary. The material must be optically thin to proton radiographs and have high ballistic performance

to protect the vessel from leakage. To determine if a material provides quality radiographs one could calculate the Scattering Angle, Blur, and Radiation length (SABR) for the material (for a detailed description see the section labeled proton radiography). To compare the ballistic efficiency of the armor the ballistic limit velocity, depth of penetration or energy/crater volume vs. velocity comparison methods may be implemented [M. Hackett 2001]. To make the comparison easier a quality factor Q_f has been suggested that addresses both radiographic quality and ballistic efficiency (see proton radiography for a detailed description). Based on data collected from Wilkins 5th light armor report one can construct a graph of trends for various ceramics as depicted in figure 2. At any given projectile velocity the ceramic with the highest quality factor would be the best choice. It should be emphasized that the ballistic limit velocity would be calculated for a particular threat varied only by impact speed, it is therefore necessary to have a clear definition of the expected threat.

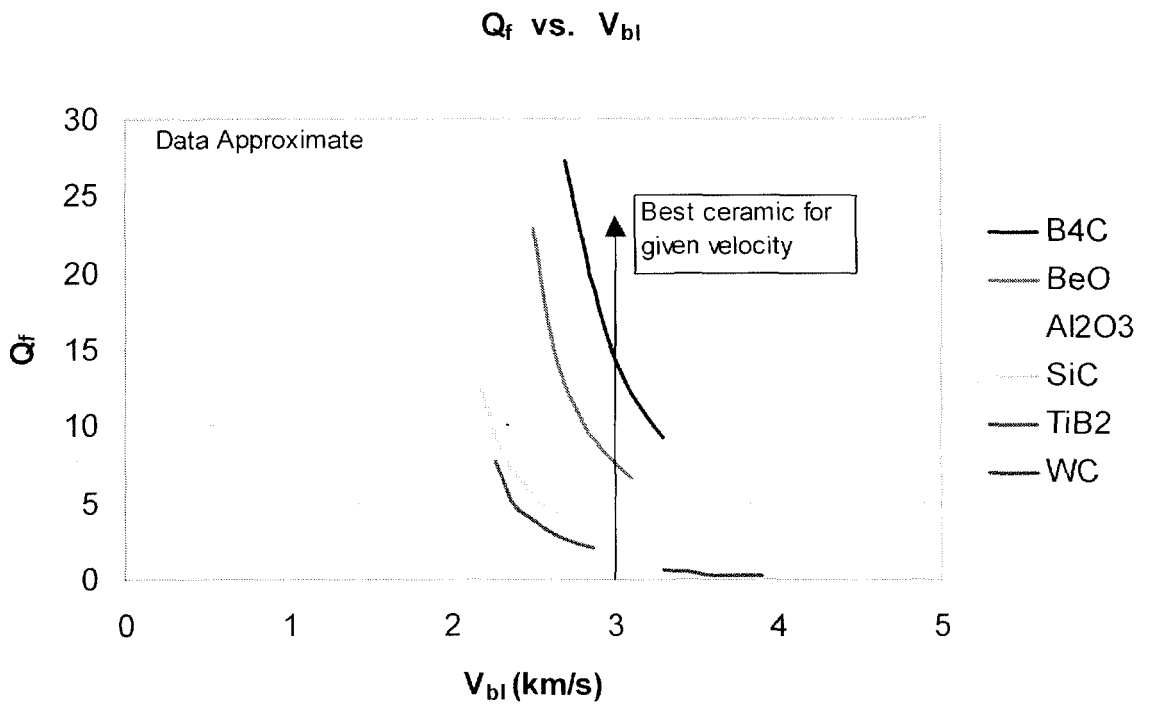

Figure 2: Expected trends for ceramic quality factor vs. its ballistic limit velocity

Although our vessel may see a variety in the type of threat there may be distinct regions where one type of threat is seen much more than another. If this is the case we may choose to use 2 or 3 different types of armor.

Consultation

Dr. Mark L. Wilkins has done ground breaking research in the field of armor ceramics. We felt it necessary to at least consult with him and hear his suggestions regarding the protection of our vessel. We met with him on June 19th of 2002, the following are the paraphrased comments and suggestions we received from him.

1. Fragment size, shape and velocity scatter will decrease with the use of a ceramic shield because the projectile will yield or fracture. The ceramic should force the fragments to hit the aluminum backing in a uniform manner such that scatter is reduced (i.e. the ceramic will "homogenize" the fragment spread).
2. Wilkins suggested catching the fragments in water or a soft material to try and collect primary fragment size and shape.
3. Over all the perceived 3-step plan sounds good.
4. Wilkins suggests that the beryllium based compounds would be the best if indeed we don't have to worry about the toxicity level. The second choice would be boron carbide. To learn more about beryllium toxicity levels he recommends discussing it with a health physicist as it can cause an adverse reaction in the lungs.
5. He found that when a ceramic was radially confined they could tolerate more ceramic defects. They heated the ceramic to 2000 F and the ceramic cracked, the results achieved were good, however, the non-cracked ceramic was slightly better. If low-density is not a requirement, titanium might be useful. Also, using one type of ceramic to homogenize the fragments and another to stop them should be considered.
6. A ballistic aluminum such as 7039 should be used, if possible, instead of 6061-T6.
7. Glass is another possible armor. Bruce Morgan studied shock wave effects on glass and might remember some of this information.

Although another ballistic aluminum might perform better we are limited by the weldability, forgeability and availability. The theory of using a ceramic to 'homogenize' the fragments is quite appealing and should be validated by gun tests.

Code Analysis

Dr. Wilkins does not recommend relying solely on using computer codes to model, analyze and predict armor behavior. We believe this type of analysis will produce qualitative results that will be useful. Although our exact problem has not been modeled, a few codes have been found that may be able to provide insight and understanding. A brief introduction to each is presented along with a sensitivity study of one of the codes.

The Walker-Anderson Penetration code was developed by James D. Walker, Ph.D., and Charles E. Anderson, Jr., Ph.D. at Southwest Research Institute in San Antonio Texas. The code was originally designed to model metal projectiles penetrating metal armor, a more thorough description and example set provided by Dr. Anderson is reproduced in appendix A.

Ceracode is a brittle fracture model suggested by Dr. Mark L. Wilkins, and developed by Murphy et al. This model was implemented in HI-DYNA2D and test problems were run that seemed to correlate well with experimental tests. For more information see CERACODE – A Model for Numerical Analysis of Warhead Interaction with Ceramic Armour [4].

Autodyn is a massive code that may be useful and has many capabilities above and beyond our particular problem. More information can be gathered from Century Dynamics [5].

C-ALE is a code that was developed at Lawrence Livermore National Laboratory and may be useful. To give the author a brief introduction to the code and modeling processes a sensitivity study was run under the close instruction of Ed Kokko. Although it may prove useful in the future there are many variables that affect the shrapnel-armor problem. This study was done to briefly familiarize the author with the code.

The goal of this study was to see how a projectiles incident velocity and the ceramics maximum allowable compressive stress influenced the depth of penetration. In the trial, a tungsten carbide blunt projectile impacted a titanium diboride ceramic plate 10 centimeters thick. The projectiles incident velocity and the ceramics maximum principle compressive stress to failure were varied and the resulting depth of penetration was measured. Figure 3 shows a series of time steps where the incident velocity was 2 km/s (.2 cm/μs) and the maximum compressive stress was 10 Gpa.

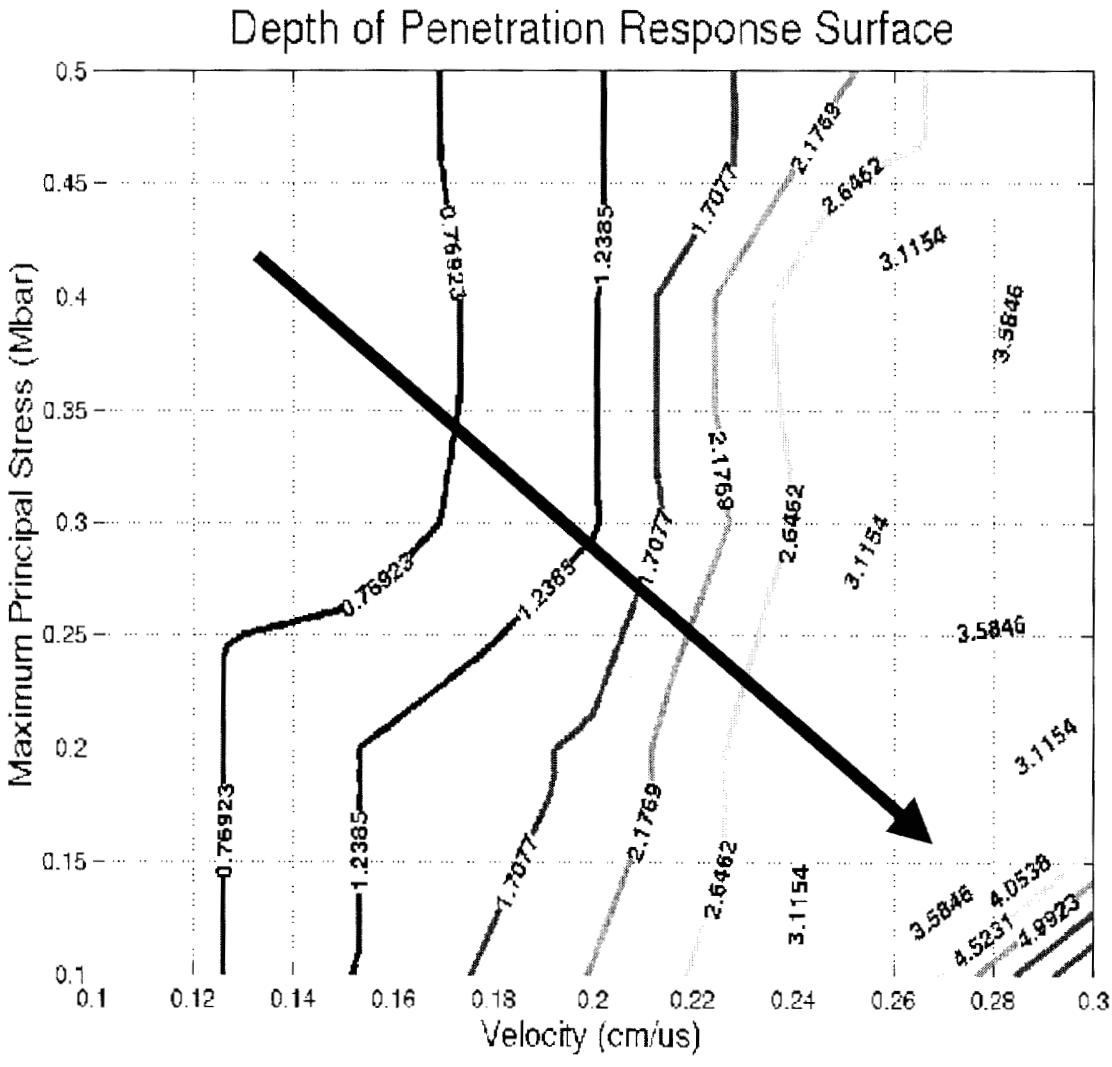

Figure 4: Response contour map showing velocity on the x-axis and principle compressive stress on the y-axis. The black arrow shows the direction of increasing depth of penetration.

As the velocity is increased by a factor of three, there is roughly a ten fold increase in depth of penetration. At each velocity the stress was varied over a range of .5 Mbar and only a slight change in depth of penetration was noticeable. These preliminary findings suggest that the accuracy of a model using this setup is more dependent on an accurate representation of the projectiles velocity and less so on the maximum compressive stress capability of the ceramic.

Proton Radiography – SABR Factors

To produce radiographs, a beam of protons, neutrons or electrons pass through a material and strike a detector. The amount of information each radiograph can provide depends on a variety of factors. The main diagnostic tool of the Advanced Hydrotest Facility is proton radiography and will therefore be the focus of this section.

Proton radiography presents a unique set of challenges that are better described in chapter two of the Los Alamos report LA-UR-98-1368. To obtain quality radiographs one needs to consider multiple coulomb scattering (MCS), blur and radiation length. A tool, SABR Factors (Scattering Angle Blur and Radiation length Factors), was designed to help aid AHF designers in choosing materials that will provide quality radiographs and is presented here.

SABR is an Excel spreadsheet and its main purpose is to calculate radiation length and coulomb scattering for user defined compounds. A description of the available features are listed below along with assumptions and equations used in the calculations. All standard values (density, atomic weight and mass) for the elements were taken from the 14th edition of Lange's Handbook of Chemistry when listed. Otherwise, data was compiled from the website *webelements.com*.

On the sheet labeled Elements, the intrinsic and specific radiation length, atomic number and weight, along with the variables in the radiation length equation are listed for every element. The footnotes provide the temperatures at which the density values were taken. If an element does not refer to a foot note, the density was taken at room temperature.

The sheet labeled Compounds is interactive and allows the user to define materials by the chemical makeup. If you click on any cell in the 2nd row of this sheet a small information box will appear giving a brief description of the values required or produced in that cell. There is currently enough space allocated for 147 different compounds, if more space is needed it is easy to add more room. The required fields (name of compound, density, thickness, and chemical compositions) are highlighted in blue, if provided this sheet will return: the intrinsic and specific radiation length using an equation and an approximation, the error between the two methods, the Coulomb scattering, blur, quality factor and areal density. To enter the chemical composition note

the list of elements in order of atomic number located in columns T through EG. Simply enter the number of atoms for each element needed to make up one molecule of your compound. For example boron carbide has 4 boron atoms for every carbon atom, thus a 4 would be entered in the column labeled boron and a 1 would be entered in the column labeled carbon. The name is a required field, the results are not visible without it, the density is necessary for all fields except intrinsic radiation length. An assumed thickness is automatically displayed when the name is entered but any thickness may be entered. When a compound and its corresponding information is entered that produces an x/X_o value outside the appropriate range ($10\text{-}3<x/X_o<100$) the results turn a bold red

Radiation Length

"[Radiation length] is the mean distance over which a high-energy electron loses all but 1/e of it's energy by bremsstrahlung, and the e-folding distance for pair production by a high-energy photon is $(7/9)*X_o$." Particle Physics Booklet (July 2000)

Although there is only one variable set aside for radiation length (X_o) it is reported in two different units. The most commonly used unit is g/cm^2. When reported in this form the radiation length is an ***intrinsic (i)*** property of the element or compound and throughout this paper will be referred to as such. The radiation length is also reported in the unit of cm. When reported in this unit the density of the element or compound must be specified and will from now on be referred to as the ***specific (s)*** radiation length. The value is density dependent, as density is not an intrinsic property, neither is the radiation length when reported in this manner.

This workbook calculates the radiation length of elements with two different equations. The first is an equation developed by Y.S. Tsai, equation 1, (Particle Physics Booklet, July 2000, pg194, eq. 23.17) and is denoted in the workbook by the label eq.

$$X_o = \frac{1}{4\alpha r_e^2 \frac{N_A}{A}\left\{Z^2\left[L_{rad} - f(Z)\right] + ZL'_{rad}\right\}} \qquad (1)$$

Where:

$$f(Z) = a^2\left[(1+a^2)^{-1} + 0.20206 - 0.0369a^2 + 0.0083a^4 - 0.002a^6\right] \quad (2)$$

X_o = radiation length

α = fine structure constant

r_e = the radius of an electron

N_A = Avogadro's number

A = the atomic weight of the element (g/cm^2)

Z = the atomic number of the element

$a = \alpha Z$

L_{rad} and L'_{rad} are given in the table below.

Element	Z	L_{rad}	L'_{rad}
H	1	5.31	6.144
He	2	4.79	5.621
Li	3	4.74	5.805
Be	4	4.71	5.924
Others	>4	$\ln(184.15*Z^{-1/3})$	$\ln(1194*Z^{-2/3})$

Source: Particle Physics Booklet, July 2000, pg 195.

The second method used to calculate radiation length is an approximation provided by Dahl (Particle Physics Booklet, July 2000, pg. 195, eq. 23.19) and is denoted in the workbook by the label ap:

$$X_o = \frac{716.4\ g/cm^2\ A}{Z(Z+1)\ln\left(287/\sqrt{Z}\right)} \quad (3)$$

Where the variables are the same as those defined above. This approximation should be accurate to within 2.5% for all elements except helium.

Coulomb Scattering

When comparing materials for use in the AHF project, multiple Coulomb scattering affects the visibility of the target. When a charged particle travels through a medium the nuclei is scattered many times over small angles. If we assume the particle is traveling in the z direction in a symmetric beam (as depicted in Figure 1) and passes through a medium it will be displaced off of the z-axis by some angle θ (equation 4).

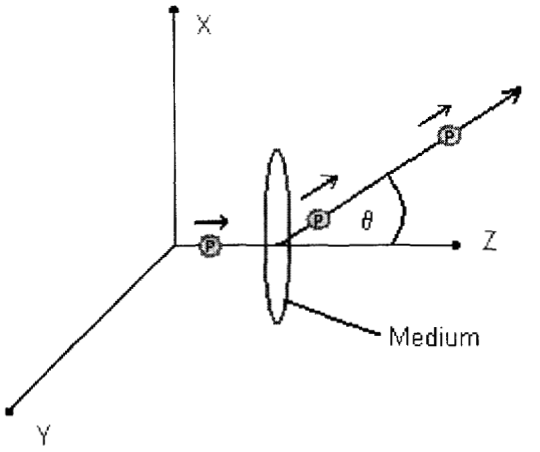

Figure 5: A proton (green) initially travels along the z-axis when it passes through a medium (blue), the proton experiences Coulomb scattering and its direction is altered to some small angle θ off of the z-axis.

$$\theta = \theta_o \times \sqrt{2} \qquad (4)$$

The square root of 2 factor applies to the root mean square angle in Gaussian approximation

Where:

θ = the root mean square angle the charged particle is displaced from it's original direction of travel

θ_o = the root mean square displacement angle projected onto the x or y axis (see below)

The projection of this angle onto the x and y-axes, θ_o, can be calculated by a gaussian approximation, equation 5. The angle on the x-axis should be equal to the angle on the y-axis because we assumed a symmetric beam on the z-axis.

$$\theta_o = \frac{13.6MeV}{\beta cp} z\sqrt{x/Xo}\left[1 + 0.038\ln\left(x/X_o\right)\right] \tag{5}$$

Where:

θ_o = the root mean square displacement angle projected onto the x and y axes

z = charge number (1 for protons)

x = thickness of material

X_o = radiation length in the same units as x

c = speed of light

β = the ratio of the speed of the particle to the speed of light and is dimensionless. It is defined by equation 6, which for our project may be approximated by the number 1.

$$\beta = \frac{\left[(1876.54 + T)T\right]^{1/2}}{T + 938.272} \tag{6}$$

for T = kinetic energy of particle divided by MeV (50 GeV protons = 50,000 MeV protons)

p = the momentum of the particle and is defined by equation 7 below, the units are MeV/c where c is the speed of light. Please note p has not been divided by the number c and is just carrying it along as a unit.

$$p = \left(\sqrt{(1876.54 + T)T}\right) * MeV/c \tag{7}$$

where T/MeV is unitless and T is the kinetic energy of the particle

This value of θ_o is from a Moliere distribution for singly charged particles. Accuracy is 11% or better for $10^{-3} < x/X_0 < 100$.

Adding materials – in Gaussian approximation, one may add according to the following form

$$\theta_o = \frac{13.6MeV}{\beta cp} z \sqrt{\sum_i x_i / Xo_i} \left[1 + 0.038 \ln\left(\sum_i x_i / X_{oi}\right)\right] \quad (8)$$

Blur

Blur is the displacement of a proton from where it is supposed to be. It is calculated as:

$$\Delta x = \theta_o \times d \quad (9)$$

Where:

Δx = the root mean square blur

θ_o = the root mean square projected angle on the x-y axis (equation 5)

d = the distance the medium is from the target (in our case the distance the vessel wall is from the nuke mock up). This variable is located in cell G158 on the compounds sheet and is currently set at 1 meter.

Quality Factors

When comparing radiographic transparency of materials a dimensionless quality factor is used:

$$Q_f = \frac{X_o}{\rho x} \quad (10)$$

Where:

X_0 is in units of g/cm^2 (intrinsic)

ρ = the density of the material in g/cc

x = the thickness of the material to be used in units of cm

Defined in this way, smaller quality factors are better. This factor accounts for Coulomb scattering in materials by dividing the radiation length by the thickness of the material. It is recommended that X_0 be obtained by equation 1, as this is more accurate. To

accurately compare the effectiveness of ceramics for the AHF project it should be assumed that the ceramic is appropriately mounted. If the thickness of the ceramic needed to stop the threat is used in equation 9 the result will accurately compare not only ceramic transparency but also shrapnel mitigation effectiveness.

Much thanks to Dr. Peter Barnes (LLNL) who has taken the time to review and revise this tool. The spreadsheet may be obtained from John Pastrnak.

Conclusion

In order to protect our vessel a strong characterization of the expected threat is necessary. Catching the fragments in soft media, using radiographs, witness plates and x-ray computed tomography are methods that will provide useful data. The armor for the AHF vessel needs to have excellent ballistic performance and be virtually transparent to protons. An effective way to compare materials for this purpose is by using the quality factor proposed, which combines the radiation length and density of the material with the ballistic thickness (the thickness needed to stop a known threat). A few possible computer codes were mentioned that may be helpful in analyzing our problem. A sensitivity study was run using C-ALE to introduce the author to the code and the modeling process. A tool was developed that will calculate the parameters relating to proton transparency if the materials chemical composition, density and desired thickness are given.

More experimental data is needed to classify our threat before any particular armor set up is chosen. This data is also needed to begin the process of the 3-step plan: that is determining the largest fragment, the deepest crater and the largest amount of energy deposition per crater. The theory of homogenizing the threat by using ceramics should be validated by a series of gun tests.

Bibliography

Methodology of Selection

1. Amy M. Waters, *Three-Dimensional Analysis of Voids in AM60B Magnesium Tensile Bars Using Computed Tomography Imagery*, Johns Hopkins University, Baltimore, Maryland, May 2001.

2. M.Hackett, *Ceramic Shrapnel Mitigation Materials in Support of the AHF Containment Vessel*, Oregon State University and Lawrence Livermore National Laboratory, UCRL _____, September 2001.

3. Conference: Dr. Mark L. Wilkins, former Lawrence Livermore National Laboratory employee.

4. Dr. Michael J. Murphy *et al.*, *CERACODE – A Model for Numerical Analysis of Warhead Interaction with Ceramic Armour*, 14th International Symposium on Ballistics Quebec, Canada, 26-29 September 1993

5. Century Dynamics Incorporated:
   http://www.century-dynamics.co.uk/index.htm
   Telephone: 925-771-2300

SABR Factors

6. LA-UR-98-1368

7. 14th edition of Lange's Handbook of Chemistry

8. webelements.com

9. Particle Physics Booklet (July 2000)

Appendix A

An Analytical Penetration Model

Southwest Research Institute
San Antonio, TX 78228-0510

The Walker-Anderson Penetration Model was initially developed to predict the time-dependent penetration of long-rod projectiles into semi-infinite metallic targets. The model is based on integrating the momentum equation along the centerline of the project-target centerline, combined with assumptions concerning the three-dimensional flow field within the target. The model has been shown to be very robust and quite accurate for other projectiles besides long rods.

The model has been extended to include finite-thickness effects, including bulging and perforation. In particular, two bulging/perforation models are available: (1) a first-principles bulging model (bulging develops directly from the plastic flow field), and (2) a geometric bulging model. There are advantages and disadvantages to both descriptions. It is almost always preferable to use a first-principles model when available. However, to date, failure modes within the first-principle model are limited. The geometric bulging model has been shown to be quite robust in many applications, and has the advantage of incorporating 6 failure modes (various types ductile, shear, and brittle shear failure). Since failure is a very complicated process, the second model can often be used with very good success to predict ballistic limit conditions.

The capability to model penetration into brittle materials (e.g., glass and ceramics) has also been developed. The penetration response into failed material is very accurate. The phenomenon of dwell, at this point, is handled in a phenomenological manner.

The Walker-Anderson model has been adapted to a user-friendly, Windows-based (Windows 2000) executable program. The program has the following capabilities:

- Semi-infinite metallic penetration ($L/D \geq 1$)
- Penetration and perforation of finite-thickness metallic targets
  - Bulging and target failure using a first-principles formulation
  - Bulging and target failure using a geometric bulge model with 6 failure modes
  - A V_{50} estimator
- Penetration of failed brittle materials (glasses and ceramics)
- Penetration & perforation of ceramic/metallic targets

Examples of the predictive capability of the Walker-Anderson model are shown on the next several pages.

For questions, please call or e-mail:

Charles E. Anderson, Jr., Ph.D. (210-522-2313; canderson@swri.edu)
James D. Walker, Ph.D., (210-522-2051; jwalker@swri.edu)

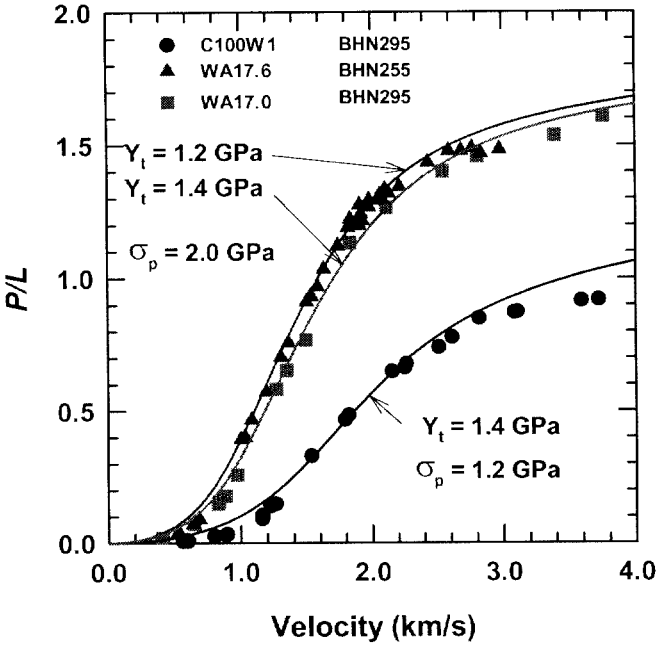

Normalized penetration vs. impact velocity for L/D 10, tungsten-alloy and steel projectiles into armor steel targets. Note that two armor steels were used for the tungsten-alloy rod experiments.

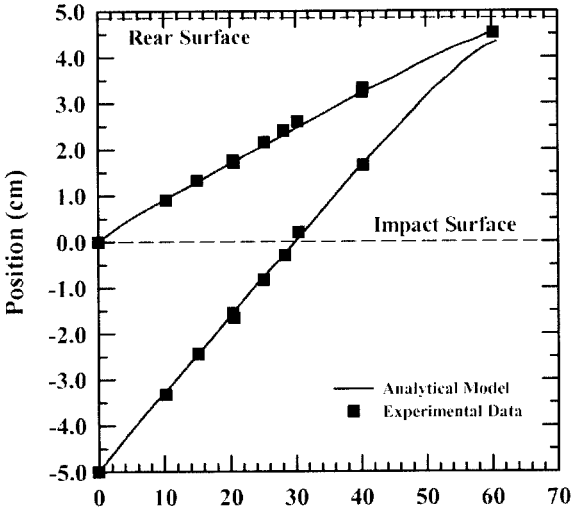

Comparison between experiments and model of the nose and tail positions.

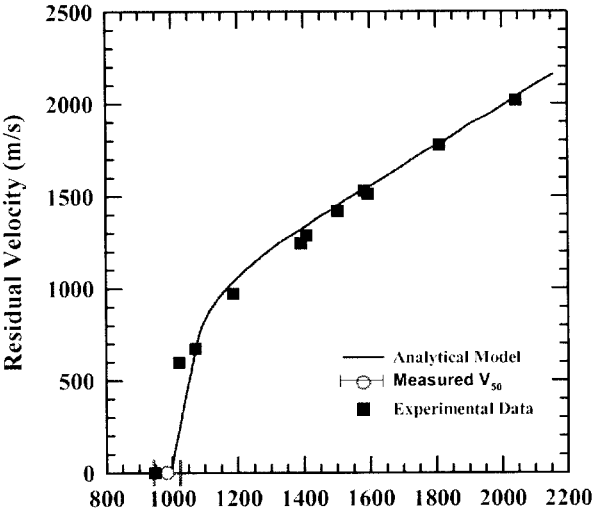

Residual velocities obtained by the model compared with experiments, including V_{50}.

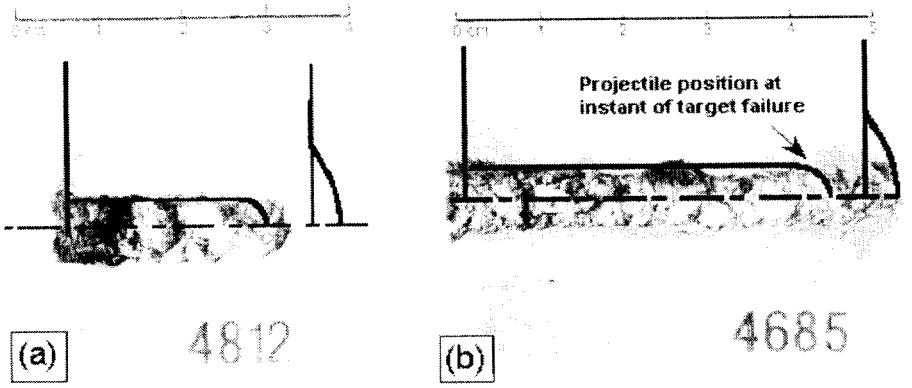

(a) V_0 = 1240 m/s, T = 2.90 cm (b) V_0 = 1680 m/s, T = 4.85 m/s

Comparison of the analytical (black line) and experimental results for bulging and perforation.

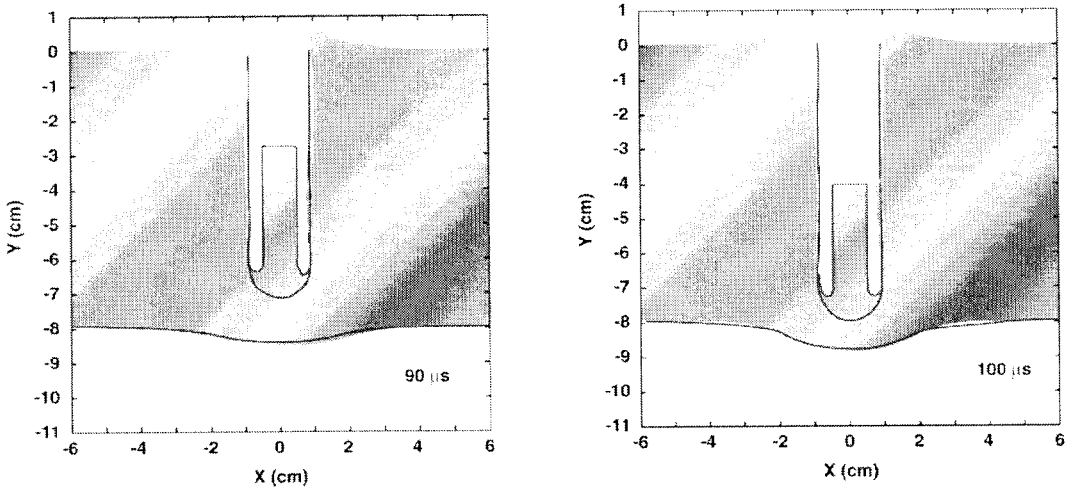

Comparison of analytic model bulging (red line) with CTH calculation (shaded region) at 90 and 100 μs. The analytic model is providing both the geometry of the projectile as well as the target.

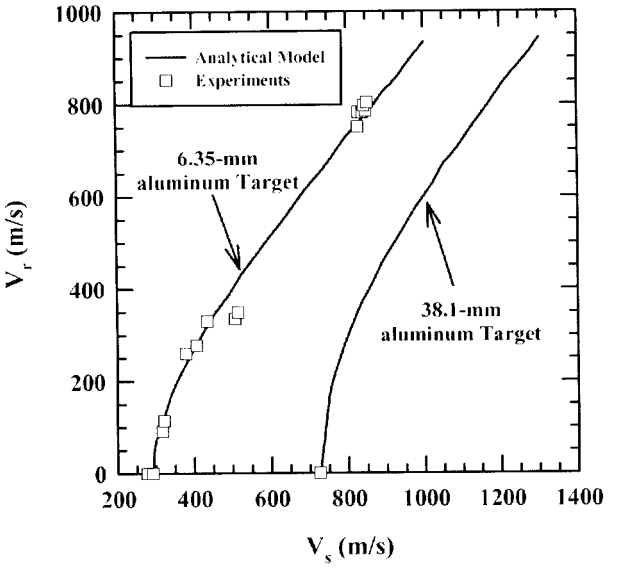

Comparison of experimental and model results for APM2 bullet into 6061-T6 aluminum.

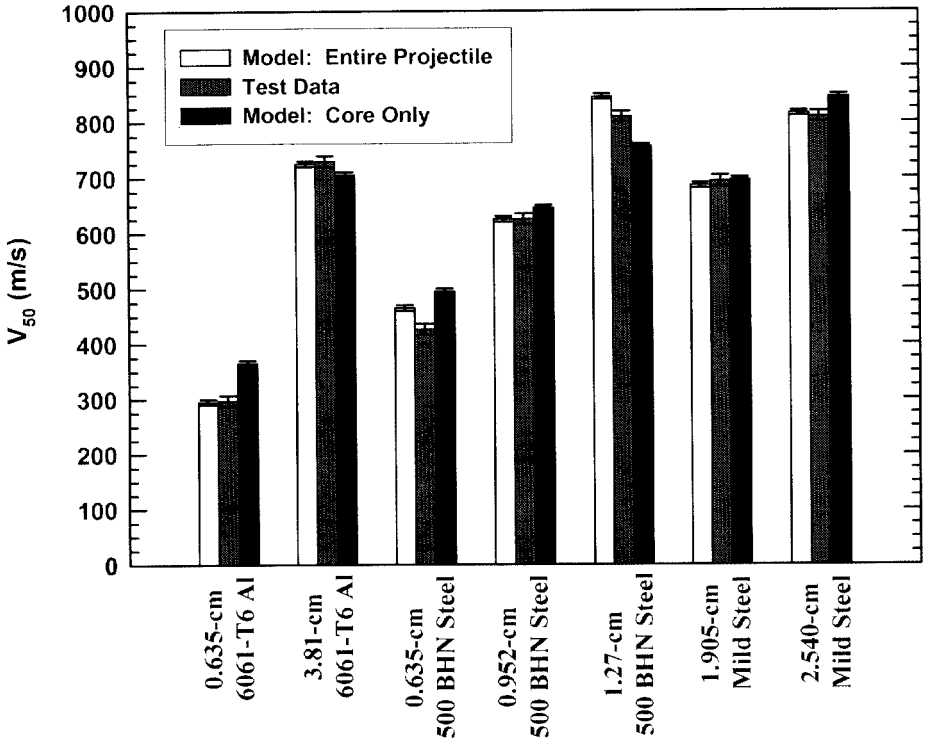

Comparison of V_{50} predictions to test data for different APM2 bullet models.

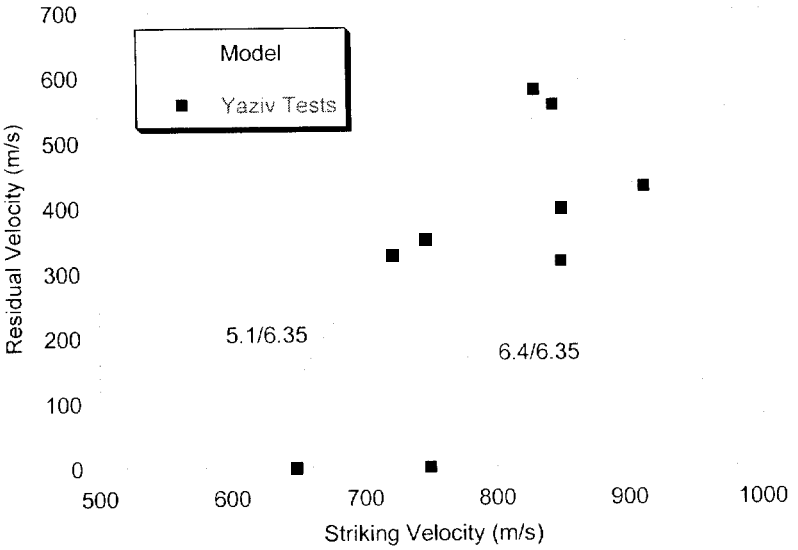

Comparison of analytical model to experimental data for V_s-V_r and V_{50} for an AP bullet into a ceramic backed by an aluminum substrate (the thicknesses of the ceramic/aluminum, in mm, are shown in the figure).

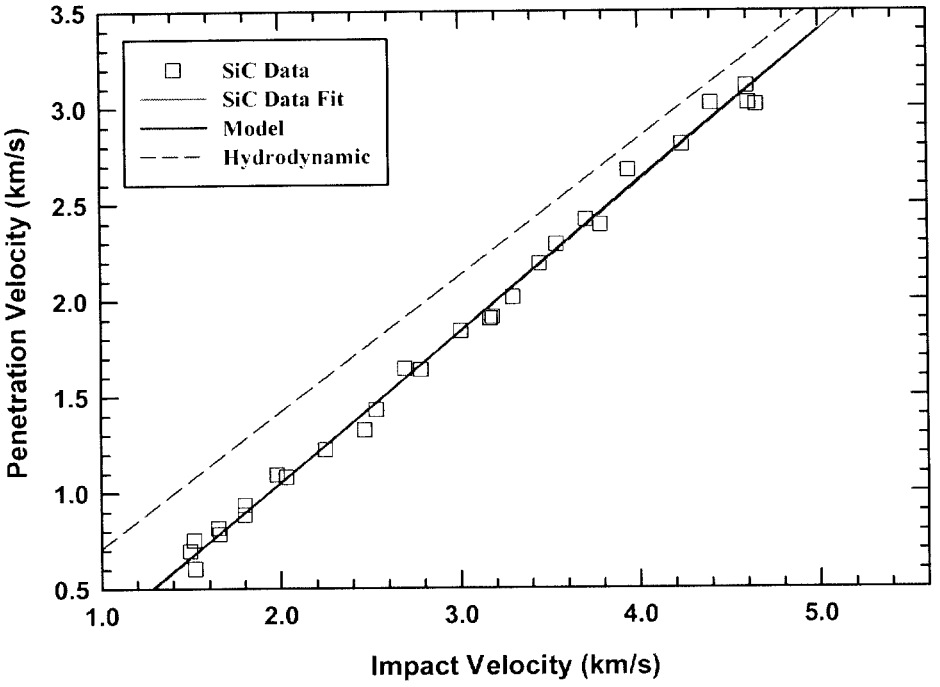

Comparison of predicted analytical model results to experimental data for penetration velocity vs. impact velocity against experimental data for SiC.

The cost of the enhanced version of the code, including user's manual, is $25,000. This can be purchased by a P.O.

As we discussed, we have a little work to do, but this can be accomplished fairly quickly.

Charlie A.
charles.anderson@swri.edu
Phone: 210-522-2313
Fax: 210-522-6290